Science of the Total Environment xxx (xxxx) 152428

Contents lists available at ScienceDirect

Science of the Total Environment

journal homepage: www.elsevier.com

Tree-ring stable isotopes indicate mass wasting processes at Radicofani in the upper Orcia Valley (Tuscany, Italy)

Giovanni Leonelli [a], Irene Maria Bollati [b,*], Paolo Cherubini [c], Matthias Saurer [c], Francesca Vergari [d], Maurizio Del Monte [d], Manuela Pelfini [b]

[a] Department of Chemistry, Life Sciences and Environmental Sustainability, Università di Parma, Parco Area delle Scienze 157/A, 43124 Parma, Italy
[b] Earth Science Department "A. Desio", Università di Milano, Via Mangiagalli 34, 20133 Milano, Italy
[c] WSL Swiss Federal Institute for Forest, Snow and Landscape Research, Zürcherstrasse 111, CH-8903 Birmensdorf, Switzerland
[d] Earth Science Department, Università La Sapienza, Piazzale Aldo Moro 5, 00185 Roma, Italy

ARTICLE INFO

Editor: Chennai Guest Editor

Keywords:
Dendrogeomorphology
Tree rings
Stable isotopes
Badlands
Shallow landslides
Orcia Valley (Apennines)

ABSTRACT

Tree-ring carbon (C) and oxygen (O) stable isotope (SI) chronologies spanning the period 1983–2012 were analysed at three *Pinus nigra* Arn. sites located in the upper Orcia Valley (Tuscany, Italy) in a badlands landscape. The goal of the study was to determine the extent to which tree-ring stable isotopes can serve as a proxy for mass wasting processes. To this end, we applied an established dual-isotope model to detect physiological changes between trees growing at three sites, one along the upper border of a well-studied shallow landslide, one on the landslide, and one in a stable area, as control. We further analysed whether trees at the three sites showed different $\delta^{18}O$ responses to climate and to precipitation $\delta^{18}O$. Tree-ring $\delta^{13}C$ and $\delta^{18}O$ variations and trends revealed impairments of the photosynthetic process at the landslide site. We found that trees growing on the landslide show signs of reduced photosynthetic capacity since the onset of the landslide in 1993, whereas since 2000, while producing compression wood during periods of landslide activity, the trees show trends of higher average maximum net photosynthesis. The correlation analysis performed between the SI chronologies and the climatic variables revealed that the climatic signals at the site located on the landslide are masked by growth stress induced by the mass wasting processes. The most distinct differences in climate responses between sites were found in tree-ring $\delta^{13}C$ in response to mean temperature and to mean temperature range, and in tree-ring $\delta^{18}O$ in response to precipitation $\delta^{18}O$. Our research confirms that it is possible to reconstruct mass-wasting processes on forested slopes and to date geomorphological events by considering the trees' physiological conditions as recorded by stable C and O isotopes in tree rings, and by comparing affected with unaffected sites.

1. Introduction

Most of the mountains and hills along the Apennine chain in Italy are characterized by clayey bedrock (Buccolini and Coco, 2013). Such slopes are affected by degradation, which can be exacerbated by different vegetation covers and land uses and by the wetting-drying cycles typical of the Mediterranean climate (Della Seta et al., 2009; Bollati et al., 2012; Brandolini et al., 2018). The changes in rainfall patterns characterized by more frequent and intense rainfall events in recent decades, have also played an increasingly significant role in degradation (Brandolini et al., 2018). The intensely dissected landscapes deriving from water runoff are known as "badlands", or as *calanchi* in Italian. They are often associated to *biancane* that are relatively small rounded hill, carved in shales and mainly related to piping action (Vergari et al., 2013a), with possible structural control of joints (Della Seta et al., 2009). A first classification of Mediterranean badlands according to climate was proposed by Gallart et al. (2002), who identified the rainfall thresholds of 200 mm/y and 700 mm/y to discriminate between arid, semiarid, and humid badlands, respectively. Landslide events affecting badlands are rather frequent and mostly triggered by intense rainfall events (Vergari et al., 2011). Within badlands, water erosion and mass-wasting operate together in a complex cause-effect mechanism, contributing to the rapid morphoevolution of these landscapes (Vergari et al., 2019).

Badlands can be categorized according to their patterns of erosion, although the mechanics and temporal patterns of the transition from one type to the next is not yet well characterized. Classic "knife-edged" type badlands have a very dense drainage pattern with channels with

* Corresponding author.
E-mail address: irene.bollati@unimi.it (I.M. Bollati).

https://doi.org/10.1016/j.scitotenv.2021.152428
Received 15 September 2021; Received in revised form 30 November 2021; Accepted 11 December 2021
0048-9697/

deep V-shaped cross profiles (type A; Moretti and Rodolfi, 2000). Badlands affected by more frequent small mass movements have gentler profiles, as sediments fill the bottom of the small valleys (type C; Moretti and Rodolfi, 2000). Badland formation can occur in relation to human impact and/or climate changes (Ciccacci et al., 2008).

Many studies of the badlands of southern Tuscany, Italy (e.g., Ciccacci et al., 2008; Castaldi and Chiocchini, 2012; Amici et al., 2017; Torri et al., 2013) have identified land-use changes (mainly farming-related activities) occurring in the second part of the 20th century as the main drivers for changes in morphodynamics. Although human activities frequently initiate or exacerbate badland formation, Brandolini et al. (2018) underlined how human interventions, that are maintained through time, can also help reduce erosion (e.g., Coratza and Parenti, 2021).

The interaction between vegetation and geomorphic dynamics can be positive or negative according to site-specific conditions (Thornes, 1985). As a positive interaction, badlands may host important plant endemic species (e.g., Torri et al., 2013), and vegetation cover may help to mitigate soil erosion (e.g., Bucciante, 1922; Gallart et al., 2013; Ballesteros Cánovas et al., 2013). On the other hand, water runoff on clayey soils may induce disturbances to vegetation (e.g., Chiarucci et al., 1995; Bollati et al., 2012; Ballesteros Cánovas et al., 2013; Bollati et al., 2016). The environmental impacts on trees may be of various natures, deriving from biological interactions or from physical processes. Physical processes may include the geomorphological ones, the extreme climatic conditions (drought stress, low temperature, etc.), fires, soil/air pollution. These impacts may affect various organs of the trees involving their physiology, causing them to divert resources for normal growth and primary metabolism to plant defense and stress metabolism (Smith, 2015). A wealth of secondary metabolism substances can be produced by trees in response to biological attacks by insect defoliators and herbivores (Herms and Mattson, 1992); in woody species, for example, tannins may reach up to 5–10% of the dry weight of leaves (Barbehenn and Constabel, 2011). Defoliation may reduce tree-ring growth and maximum latewood density, cause the formation of intra-annual density fluctuations and white rings (Schweingruber, 1996; Hogg et al., 2002; Sutton and Tardif, 2005; De Micco et al., 2016). For isolating wood decayed parts due to internal degradation processes or to scars caused by external impacts, a complex compartmentalization process for tree protection involves the production of resins, gums and tannins, and can take years to be completed (Shigo, 1984).

In cases in which geomorphic processes are not fatally destructive, trees can be a powerful tool for dating environmental and geomorphic changes with an annual resolution (Schweingruber, 1996). Specific indicators such as growth anomalies, reaction wood, eccentric growth, traumatic resin ducts, and root exposure can all provide valuable information about the evolution of a geomorphic process (e.g., Alestalo, 1971; Stoffel and Corona, 2014; Arbellay et al., 2014). Although the mechanical stress induced by mass-wasting processes and the relative signals in tree rings have been widely studied, including in the badlands context (e.g., Bollati et al., 2012, 2016; Ballesteros Cánovas et al., 2013), the physiological reaction of trees to these geomorphic processes is poorly understood. Stable isotopes reflect the physiological conditions of the trees (McCarroll and Loader, 2004), thus the signals stored in the stable isotope signature of tree rings from sites disturbed by geomorphic processes may provide important information about both tree growth and geomorphology. To our knowledge, the chemical isotopic composition of tree-ring cellulose has not yet been used to study geomorphic processes and events.

Tree-ring cellulose stable isotopes result from isotope fractionation occurring at the leaf-level during uptake and assimilation of CO_2 as well as during transpiration. Tree-ring cellulose stable isotopes have long been used to understand trees' physiological responses to climate (e.g., Saurer et al., 1997, 2000, 2016; Treydte et al., 2001, 2006; Kress et al., 2010; Tognetti et al., 2014; Bégin et al., 2015; Payomrat et al., 2018; Nagavciuc et al., 2019). However, the use of tree-ring stable isotopes in climatic reconstructions is not straightforward, as local factors such as pollution (e.g., Savard, 2010; Leonelli et al., 2012; Sensuła, 2015; Savard et al., 2020; Savard and Daux, 2020), as well as tree physiology itself, may alter the climatic signal through time. Long-term trends in the stable isotope signals could be related to tree age (Klesse et al., 2018) and species (Arosio et al., 2020).

The tree-ring cellulose stable isotopes that are most often studied are $\delta^{13}C$ and $\delta^{18}O$. The variability of $\delta^{18}O$ in tree-ring cellulose is a function of factors like the oxygen isotopic signature of the source water, which depends on seasonal precipitation, the soil-water profile, and rooting depth, as well as leaf-water enrichment during transpiration and post-photosynthetic processes (McCarroll and Loader, 2004). In climate contexts with low relative air humidity, as is the case in the Mediterranean, significant amounts of precipitation evaporate from the soil surface during the summer, which may lead to significant oxygen enrichment (Saurer et al., 2016). The physiology of different species is reflected in the cellulose $\delta^{18}O$ signal to varying degrees and depends on how sensitive transpiration is to dry conditions. The orographic conditions and soil properties of the site also influence other variables, such as source water vs. needle enrichment (Treydte et al., 2014). Relief may influence the $\delta^{18}O$ isotopic signature in precipitation, creating rain shadow effects. In Italy, air masses mainly move eastward, resulting in lighter isotopic values east of the Apennine ridge (Longinelli et al., 2006).

The $\delta^{13}C$ depends mainly on the ratio between photosynthesis and stomatal conductance, which is linked to water-use efficiency. In sites characterized by long dry periods, the ratio varies as a function of air humidity and soil water availability (Farquhar et al., 1989). The tree-ring $\delta^{13}C$ is therefore a useful indicator of summer drought in Mediterranean environments (De Micco et al., 2007; Di Matteo et al., 2010; Tognetti et al., 2014; Altieri et al., 2015). In order to better assess tree physiological conditions in response to climate or other environmental factors on a yearly basis, tree-ring $\delta^{13}C$ and $\delta^{18}O$ changes may be analysed together to determine the influence of stomatal conductance and photosynthetic capacity on the stable isotope signature (Scheidegger et al., 2000).

Because tree physiology may be affected by external environmental processes, we hypothesize that mass-wasting processes affect tree physiology, and that the related stress responses, are reflected in changes in the tree-ring stable carbon and oxygen isotopes. The selected study site is in the surroundings of Radicofani village (Central Apennines, Upper Orcia Valley, Tuscany), where badlands characterized by shallow landslides are the dominant trait. Moreover, at the site located on a landslide, we hypothesize that the climatic signals recorded in the stable isotope chronologies are masked by physiological responses to the mass-wasting processes.

2. Study area

In this study, the tree-ring stable carbon and oxygen isotopes were analysed in trees growing on a slope characterized by both water runoff and periodic shallow landslides in the surroundings of the Radicofani village (Central Apennines, Upper Orcia Valley, Tuscany). The site selected for the analysis has been studied for a long time (at least 25 years) using multidisciplinary approaches aimed at understanding and monitoring recent hillslope morphodynamics and their causal factors. The good characterization of the research site is ideal for independently testing the usefulness of stable isotopes as a new tool in this context.

The Radicofani area (Central Apennines, Tuscany; Fig. 1) is highly representative as a sub-humid temperate badlands Mediterranean area. The area underwent reforestation practices during the 1960–1970 period and the dominant species are black pine (*Pinus nigra* Arn.) and Arizona cypress (*Cupressus arizonica* Greene) (Castaldi and Chiocchini,

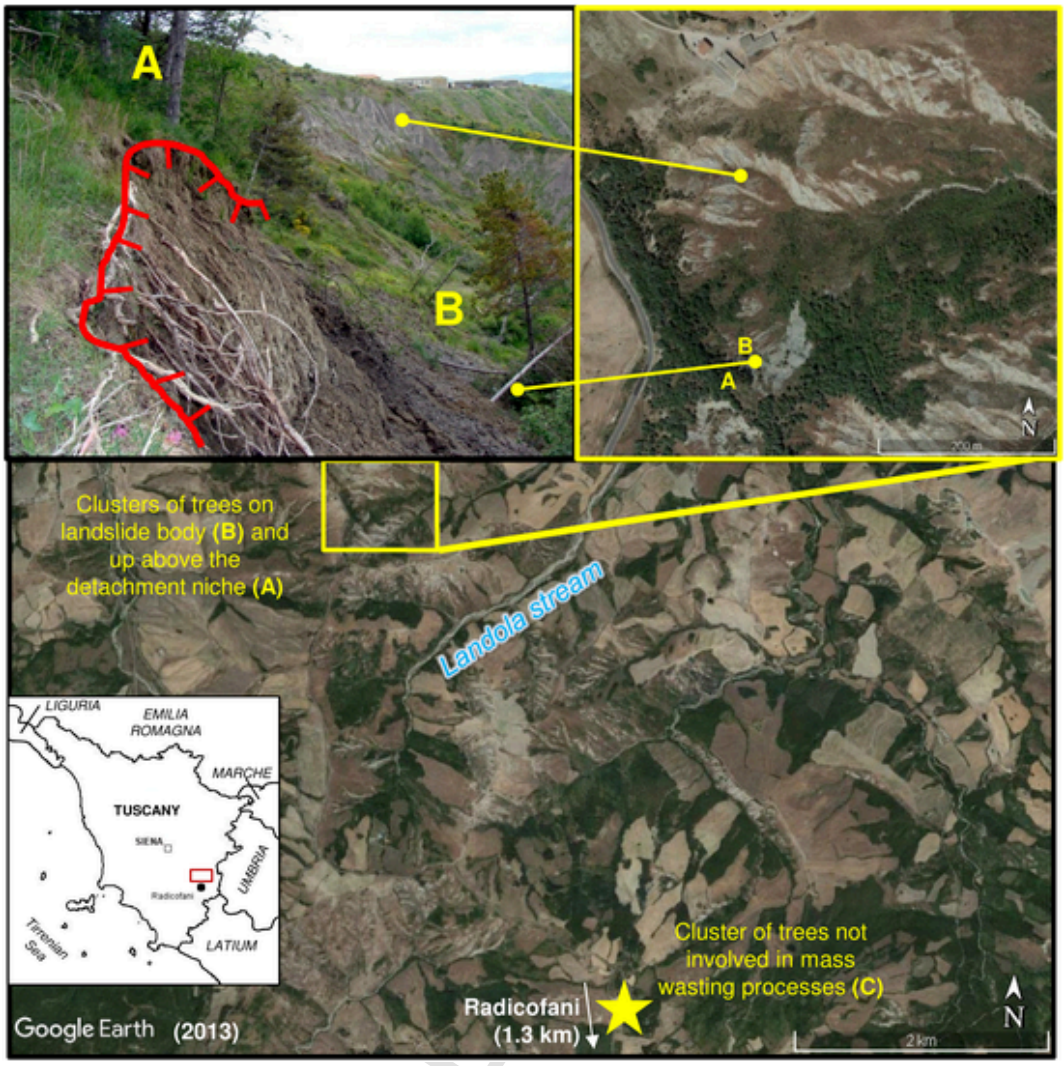

Fig. 1. Location of the study area and of the sampling clusters in the Tuscany region. The Google Earth images were taken in 2013.

2012), both of which are quite sensitive to summer droughts. Droughts in the Mediterranean area are often responsible for the intra-annual density fluctuations in tree rings (e.g., De Micco et al., 2007). Although the aim of the afforestation efforts was to reduce erosion processes, the trees are still involved in mass-wasting processes. Those that survive the mass-wasting events continue to record in their annual rings precious information about slope dynamics, as discussed by Bollati et al. (2016).

2.1. Geological and geomorphological setting

Clayey Plio-Pleistocene marine deposits outcrop widely along the Apennine; in the study area, they derived from the infilling of a NW–SE-striking graben (Carmignani et al., 1994; Belisario et al., 1999). The uplift they underwent during the Quaternary, due to pluton emplacement and widespread volcanic activity along the Tyrrhenian side of central Italy (Liotta, 1996; Acocella and Rossetti, 2002), has been particularly strong along the southern margin of the Radicofani Graben. Locally, marine deposits outcrop at 900 m a.s.l., from the neck of Mt. Amiata-Radicofani on the western slope of the study area to Mt. Cetona on the eastern slope.

Fluvial erosion, slope denudation, and gravity are major contributors to the morphogenesis of the study area. Water erosion in particular is pervasive; given the extensive clayey outcrops and the current climatic conditions, water erosion contributes strongly to the area's typical sharp- and rounded-edged badlands features.

Along the study slopes, *calanchi* predominate: the landscape in this area is very rough and the slopes are generally steep, often limiting human activities. Landslides are frequent, providing a considerable amount of material that is then transported by the major rivers of the region (Della Seta et al., 2009; Ciccacci et al., 2003, 2008; Vergari et al., 2011; Del Monte et al., 2015). Human activity in the form of deforestation, grazing, and farming has significantly affected the landscape for a long time; in recent times, cropland abandonment is also a contributor (Torri et al., 1999, 2013; Vergari et al., 2013b; Aucelli et al., 2016; Amici et al., 2017).

Previous studies indicate that the study area has undergone two main phases of geomorphological evolution, driven primarily by land cover changes and by the increasing frequency of extreme rainfall events (Ciccacci et al., 2008; Aucelli et al., 2016; Bollati et al., 2016). During the second half of the XX century, Ciccacci et al. (2008) detected a spatio-temporal geomorphological trend from type "A" (water-runoff dominated) to type "C" (where shallow landslides occur). Aucelli et al. (2016) calculated a slight decrease in the average water erosion rate during the last 60 years, accompanied by a parallel increase in the frequency of mass-wasting events. The same trend was verified by Bollati et al. (2016) using dendrogeomorphological indicators in tree rings like growth anomalies, reaction wood, and root exposure. That analysis revealed that recent landslide reactivation episodes along the slope (i.e.,

1993, 1997, 2000, 2005, 2011) triggered an intensification of suffering in trees as recorded by dendrogeomorphological indicators like reaction wood and growth anomalies. Two main phases were described: i) from the mid-1980s to the mid-1990s, water runoff was exacerbated in the area and growth suppression was detected mainly in trees located immediately to the north of the landslide body (A, in Fig. 1) where this process is dominant; ii) from the mid 1990s until 2012, growth suppression occurred in trees located on the landslide body after the 1993 event, and especially after the 2000 event while reaction wood continuously affected the bent trees.

Calanchi are considered hot-spots of erosion (Della Seta et al., 2009) because erosion rates in these areas are at least an order of magnitude greater than elsewhere (e.g., Alexander, 1982; Ciccacci et al., 2003; Clarke and Rendell, 2006). At the Radicofani site, the calculated erosion rates range from 1.65 cm/y (Della Seta et al., 2009) to 7.5 cm/y considering gravity contributions (Ciccacci et al., 2008). On slopes dominated by water runoff, the denudation value obtained by Bollati et al. (2016) by means of dendrogeomorphology is 1.61 cm/y. Where landslides dominate, erosion rates reach 11.87 cm/y, confirming the temporal trend from *type A* to *type C*, which aligns with data coming from remote sensing (i.e., 15 cm/y; Aucelli et al., 2016; Neugirg et al., 2016).

2.2. Climate setting

Meteorological data were taken from an Automated Weather Station of the National Centre for Aeronautical Meteorology and Climatology located in the town of Radicofani, about 6 km away from the sampling area. The area is characterized by a temperate warm climate, with typical Mediterranean temperature and rainfall trends.

Over the 30-year period of analysis (1983–2012), the mean annual temperature is approximately 12 °C, and mean monthly temperature show a maximum in July (23 °C). The mean annual precipitation over the same period is 937 ± 216 mm (±1σ), with a monthly minimum in July (35 mm) and two local maxima in April (82 mm) and November (152 mm) (Fig. 2). These values allow us to categorize the studied badlands area as *humid-* or *wet-type* (sensu Gallart et al., 2002 modified by Nadal-Romero et al., 2021). The main precipitation peak occurs during autumn, following the semi-arid conditions of summer, during which approximately 30 days of drought occur between July and August. According to Vergari et al. (2013b), the two main rainfall peaks in April and November favour strong runoff erosion and shallow landsliding, respectively. The area is particularly prone to landsliding, when the bedrock is saturated from the autumn and winter rainfall seasons.

3. Methods

The *P. nigra* trees investigated in this study were planted because they grow well in this environment and are suitable for reforestation efforts aimed at reducing soil erosion. To determine whether stable isotopes (i.e., $\delta^{18}O$ and $\delta^{13}C$) can be used as a proxy for mass-wasting processes, and in particular for understanding temporal variations in water-related geomorphic processes, 40 trees were sampled in June 2013 (Bollati et al., 2016). Samples were collected from trees growing in three distinct clusters (Figs. 1 and 3):

- Site A) Trees located immediately above the detachment scarp of the 2013 landslide;
- Site B) Trees located on the landslide body, that was dissected in different portions, some of which were carried downslope during the event; This cluster corresponds to the *Group 2* described in detail by Bollati et al. (2016);
- Site C) Trees located about 4.5 km away from the disturbed slope, influenced by neither water runoff nor by gravity processes. This is the control group.

In the disturbed area, a total of 40 trees were sampled by taking three cores per tree at 1.3 m above ground using a Pressler increment borer. In the control area, a total of 15 trees were sampled in the same way (see Bollati et al., 2016). To avoid any disturbance of the stable isotope signal, the samples for this analysis were extracted from the portion of the trunk not affected by compression wood (i.e., up-valley and far from curved sections of the trunks). The extracted cores were visually cross-dated under a microscope for eliminating potential dating errors, and checked for avoiding rings with compression wood, and cores from the same tree were compared with one another. Then, annual

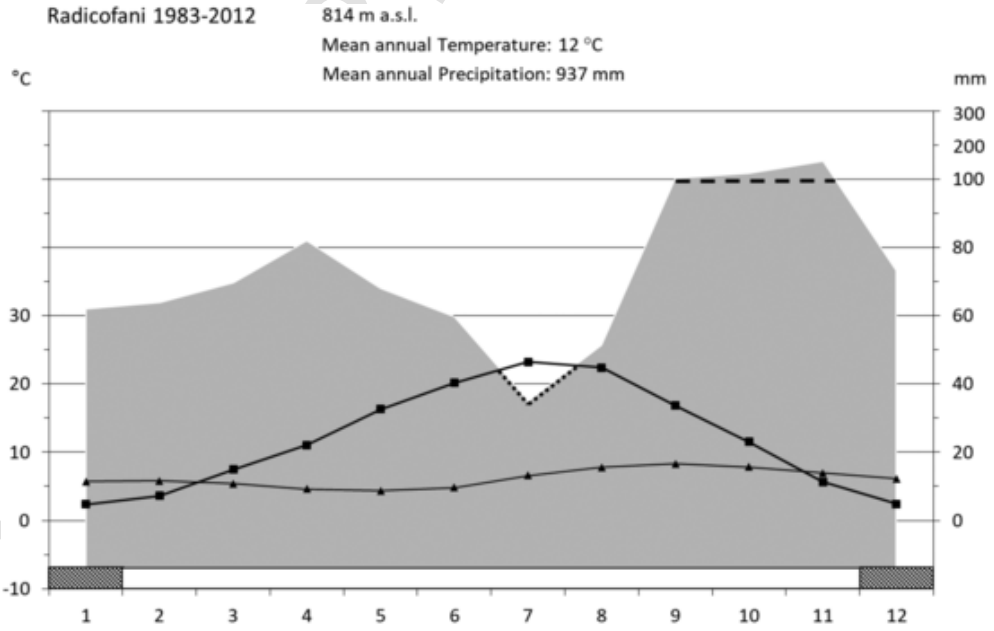

Fig. 2. Ombrothermic diagram of the Radicofani Automated Weather Station. Meteorological series refer to the 30-year time period over which the analyses of tree-ring stable isotope responses to climate were performed (1983–2012). The dotted line of precipitation depicts periods of drought, whereas the dashed line depicts periods of abundant precipitation (above 100 mm/month). The line with square dots depicts the mean monthly temperature, whereas the line with triangle dots depicts the monthly mean temperature range. The grey blocks at the bottom of the chart depict periods of possible frost.

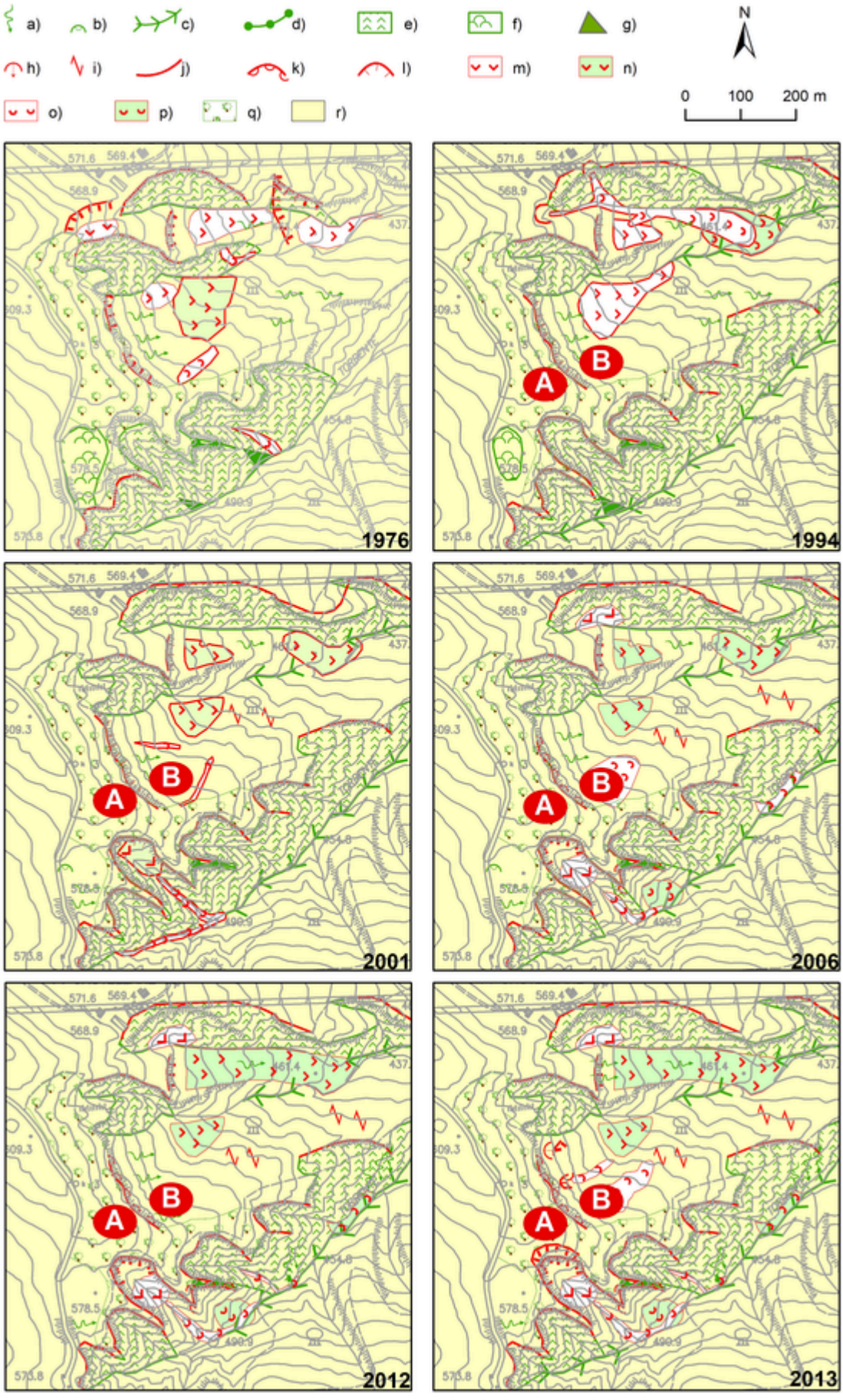
a)
b)
c)
d)
e)
f)
g)
h)
i)
j)
k)
l)
m)
n)
o)
p)
q)
r)
N
0 100 200 m
1976
1994
2001
2006
2012
2013
A
B

Fig. 3. Geomorphological sketches depicting the evolution of the investigated slope from 1976 to 2013 (year of sampling). Sampling sites A and B are highlighted. a) Surface affected by rill erosion; b) single biancana; c) V-shaped valley; d) sharp ridge; e) calanchi badlands; f) area affected by biancana badlands; g) small fluvial erosion facet; h) small landslide; i) soil creep; j) polygenic scarp; k) earth flow scarp; l) earth slump scarp; m) earth slump body; n) vegetated earth slump body; o) earth flow body; p) vegetated earth flow body; q) forest cover; r) clayey and sandy clayey (Pliocene) outcrop.

rings were separated from one another with a razor blade with the objective of obtaining stable isotope chronologies with an annual resolution for the time interval 1983–2012. In order to have enough material after the cellulose extraction, tree rings from the same year were pooled together for each sampling site. In total, three sets of 30 samples each were processed for measuring the cellulose $\delta^{18}O$ and $\delta^{13}C$. The samples were milled to a fine powder (0.05 mm in diameter), resulting in 9.9–10.0 mg for the α-cellulose extraction. This last phase was performed according to the method described in Loader et al. (1997). The weight of cellulose put into the silver capsules ranged from 0.900–1.000 mg. The samples were then converted with a high-temperature pyrolysis system and the resulting gases analysed with an isotope ratio mass spectrometer IRMS (Delta V Advantage, Thermo, Bremen, Germany) with a precision greater than 0.2‰ (Weigt et al., 2015). The $\delta^{13}C$ raw series for all sites were corrected (McCarroll and Loader, 2004) in order to account for anthropogenically-induced changes in the $^{13}C/^{12}C$ of atmospheric CO_2.

3.1. Data analysis

Both the corrected $\delta^{13}C$ and the $\delta^{13}O$ chronologies were transformed into z-scores and then analysed in pairs of $\delta^{13}C$ and $\delta^{18}O$ series for each site. Moreover, at the three sites, a simple index given by the Standardized Carbon to Oxygen Difference (SCOD) was computed for all n-years as follows:

$$SCOD_n = \left(\delta^{13}C_{z-score}\right)_n - \left(\delta^{18}O_{z-score}\right)_n$$

SCOD allows us to track year by year changes in trees' physiological conditions induced by changes in stomatal conductance and photosynthetic capacity, following the conceptual model of Scheidegger et al. (2000). This index assumes values close to 0 when both $\delta^{13}C$ and $\delta^{18}O$ show similar values, indicating either enhanced stomatal conductance (both isotopic values are positive) or a reduced stomatal conductance (both isotopic values are negative). When the SCOD index assumes values that are greater in absolute terms than fixed threshold values around 0, i.e., if the index values are positive, it indicates a high photosynthetic capacity in trees (high $\delta^{13}C$ and low $\delta^{18}O$). In contrast, if the index values are negative, the trees have a low photosynthetic capacity (low $\delta^{13}C$ and high $\delta^{18}O$). It should be noted that changes in source water and physiology over time could be recorded in the tree-ring $\delta^{18}O$, a possibility not accounted for in the semi-quantitative Scheidegger model (Roden and Siegwolf, 2012).

We performed a correlation analysis between the stable isotope chronologies and meteorological variables for the period 1983–2012 using data from the above-mentioned meteorological station in Radicofani. Monthly and seasonal variables from $March_{-1}$ ('−1' indicates a variable in the year prior to growth) to September of the year of growth were computed for mean temperature, mean temperature range (calculated as the difference between maximum and minimum mean monthly temperature), and total precipitation.

A series of precipitation $\delta^{18}O$ from Porano (approximately 36 km SE of the study area) was also developed to detect the influence of precipitation isotopic signature on tree-ring stable isotopes at the study sites, based on measured data of surrounding stations and gap-filling. The reconstructed series was based on data from the following 9 stations of the Global Network of Isotopes in Precipitation (GNIP; IAEA/WMO, 2021), located on the Italian peninsula (from N to S): Bologna (Cnr), Genoa (Sestri), San Pellegrino in Alpe, Pisa (Central), Porano, Subiaco Santa Scolastica, Campo Staffi, Fogliano, and Zannone Island. Except for the Bologna station, all stations are to the west of the Apennine ridge and located within 330 km of Porano. The selected series all have at least 26 months of data (mean 58 months) over the 21-year period from 1982 to 2003. The original Porano series (September 2000–September 2003) was therefore extended back to January 1982 on monthly basis, considering regional average departures based on all stations. From January 1982 to August 2000, 9 missing values of regional departures out of 224 (i.e., 4%) were estimated using the value of mean departure for the month. A correlation analysis between the stable oxygen isotope chronologies and the Porano precipitation $\delta^{18}O$ series was performed for the period 1983–2003 using monthly and seasonal variables from $March_{-1}$ to September.

4. Results

4.1. The isotope chronologies and the SCOD index

The constructed $\delta^{13}C$ and $\delta^{18}O$ chronologies span the period 1983–2012 and show similar mean values and interval trends over some periods, underlining a common influence of climate. Similar patterns are observed, e.g., at sites A and C for the periods 1995–2002 for $\delta^{13}C$ and 1983–1997 for $\delta^{18}O$ and at sites A and B for the period 1983–1999 for $\delta^{18}O$ (Fig. 4A). However, some differences arise between sites that can be traced back to the different geomorphological settings where the trees are growing. The overall mean correlation between the chronologies is rather low for carbon ($r = 0.17$ for $\delta^{13}C$) and more significant for oxygen ($r = 0.49$ for $\delta^{18}O$) (Table 1).

A PCA run was performed for detecting clusters in the stable isotope chronologies using the 30 years as variables and the 6 sites as samples. The run reveals an expected separation between $\delta^{13}C$ and $\delta^{18}O$ chronologies on PC1, but a higher clustering in $\delta^{13}C$ chronologies than in $\delta^{18}O$ chronologies. The $\delta^{18}O$ chronology at site C is clearly separated from those at sites A and B (Fig. 4B).

A joint analysis of the $\delta^{13}C$ and $\delta^{18}O$ z-scores reveals a clear pattern of almost always concordant interval trends at the control site C (Fig. 5A). In contrast, the landslide site (site B) often shows opposite interval trends in the $\delta^{13}C$ and $\delta^{18}O$ series (Fig. 5A). Correlation values between the two isotope series within each site range from 0.0 (site B) to 0.36 ($p < 0.05$; site C). Calculated as the difference between the z-scores of $\delta^{13}C$ and $\delta^{18}O$, the SCOD index indicates similar patterns at all sites up to 1989 (Fig. 5B). At site B, there is evidence of disturbances in the physiological process, with a strong decrease in SCOD values from 1993 to 1999 (which corresponds with high values of $\delta^{18}O$ and low values of $\delta^{13}C$; Fig. 5A). In the years 1995–1999, these SCOD values exceed -1σ standard deviation of SCOD values at the control site C (horizontal dashed lines in Fig. 5B). The SCOD values at site B also show an increasing trend since 2000 with some sudden drops in 2003 and 2011 (Fig. 5B). At site B, the values of $\delta^{13}C$ over the period 2006–2010 are higher than those of $\delta^{18}O$, with values exceeding $+1\sigma$ standard deviation of SCOD values at the control site C. At site A, differences from the control site C arise already in 1991 and 1994 (low SCOD), and in 2000, 2008, and 2010 (high SCOD). However, the general trend is similar to that observed at site B.

4.2. Relationship with climatic variables

The analysis of climate influence on tree-ring stable isotopes revealed higher correlation values with trees growing at the control site C (the one not influenced by mass-wasting processes) than with trees at the other two sites. In particular, the influence of temperature on $\delta^{13}C$ is evident for several months of the growing season, with positive correla-

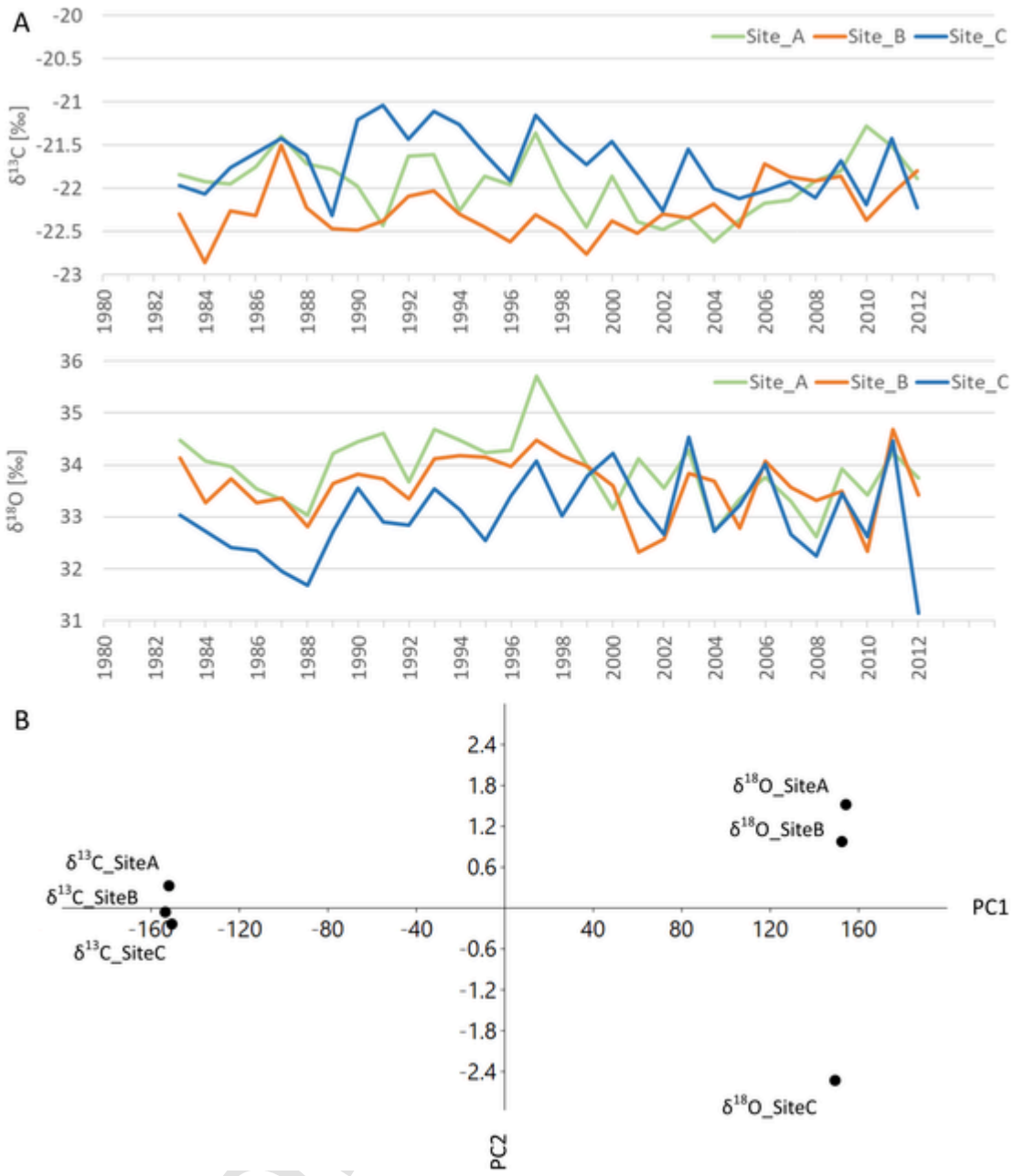

Fig. 4. A) The corrected $\delta^{13}C$, and the $\delta^{18}O$ chronologies for the three sampling sites. Site A is above the landslide scarp; site B is on the landslide; site C is a control site that is not disturbed by mass wasting. B) Scatter plot of the PCA performed to identify clusters of the stable isotope chronologies using the 30 years as variables and the 6 sites as samples.

tion values up to $r = 0.65$ ($p < 0.001$) between August mean temperature and $\delta^{13}C$ at site C (Fig. 6A). Correlation values at site A (outside but close to the landslide) are somewhat lower than at site C, except for summer months when no correlation is found. At site B (on the landslide), the influence of mean temperature is almost opposite that observed at site C. The seasonal variables also reveal an influence of the climatic conditions of the previous growing season on the $\delta^{13}C$ at sites C and B. However, the higher correlations are found for the months from March to August of the current growing season (for site C: $r = 0.54$; $p < 0.01$).

The clearest distinction between site B and the other sites is evident in the influence of the mean temperature range on $\delta^{13}C$, although the absolute values of the correlation coefficient are not very high (Fig. 6B). At the control site C, high temperature ranges tend to decrease the tree-ring $\delta^{13}C$ values, whereas low temperature ranges tend to increase the $\delta^{13}C$ values (i.e., a negative correlation exists). At this site the mean temperature range of the previous growing season has the strongest influence on $\delta^{13}C$ ($r = -0.45$; $p < 0.05$); however the highest positive correlation is found at the end of the growing season, in September ($r = 0.61$; $p < 0.001$). At site A, the same pattern in correlation values found at site C is evident. At site B, the pattern is inverted with respect to the other two sites, with high temperature ranges tending to increase the $\delta^{13}C$ values during the growing season and low temperature ranges tending to decrease the $\delta^{13}C$ values (i.e., positive correlation).

The influence of precipitation on $\delta^{13}C$ chronologies (not shown) is less distinct throughout the year, as is the influence of precipitation on $\delta^{18}O$ chronologies (Fig. 7A). No clear patterns in the correlation values emerge in either monthly or seasonal variables. However, the precipitation $\delta^{18}O$ record developed for the nearby station Porano shows positive correlation with the tree-ring $\delta^{18}O$ at site C during the growing sea-

Table 1
Correlation coefficient values between the three study sites calculated over the common period 1983–2012 for the corrected $\delta^{13}C$ and the $\delta^{18}O$ series.

	$\delta^{13}C$ Site A	$\delta^{13}C$ Site B	$\delta^{13}C$ Site C	$\delta^{18}O$ Site A	$\delta^{18}O$ Site B	$\delta^{18}O$ Site C
$\delta^{13}C$ Site B	0.28	1				
$\delta^{13}C$ Site C	0.20	0.03	1			
$\delta^{18}O$ Site B				0.57***	1	
$\delta^{18}O$ Site C				0.44	0.47**	1

*** Indicates $p < 0.001$.
** Indicates $p < 0.01$.

son (excluding August and September) (Fig. 7B). At this site, growing season precipitation (variable of months 3–7) has the strongest influence on tree-ring $\delta^{18}O$, with correlation values up to $r = 0.59$; $p < 0.01$, with May as the most influential month ($r = 0.45$; $p < 0.05$).

5. Discussion

In this article, we propose the use of tree-ring stable isotopes as a new tool in dendrogeomorphological studies. Our results demonstrate that it is possible to track and date the effects of mass-wasting processes occurring on a forested slope by analysing the trees' physiological conditions through cellulose stable isotopes. The combined analysis of $\delta^{13}C$ and $\delta^{18}O$ variations and trends at each sampling site reveals impairments of the photosynthetic process at site B, the one most impacted by the landslide. Over the period 1993–1999, high values of $\delta^{18}O$ and low values of $\delta^{13}C$ indicate a lower photosynthetic capacity compared to the control site (Scheidegger et al., 2000). The year 1993 corresponds with the onset of a first landslide event identified by Bollati et al. (2016); in this year, blocks carrying the trees started sliding downslope. The physiology of the trees was therefore impacted by the geomorphological processes and likely also by the changed soil water conditions. The trees on the landslide experienced lower photosynthetic rates until 1999, as evidenced by their significantly negative SCOD values (i.e., low $\delta^{13}C$ and high $\delta^{18}O$ values; Fig. 5B). A period of high geomorphic disturbance and compression wood production started in 2000 (Bollati et al., 2016). The stressed trees at site B showed higher photosynthetic rates at this time, as evinced by their significantly positive SCOD index values. The positive trend in SCOD values was interrupted in 2003 (a year of extreme climatic conditions during summer due to the heatwave over Europe; Beniston, 2004) and in 2011 (due to landslide reactivation along the slope) (Fig. 5B). We focus our discussion mainly on changes in photosynthetic rates because the general climate setting is rather wet. Changes in stomatal conductance cannot be excluded based on the Scheidegger model, but are expected to be less significant. Our results at site B indicate an acceleration of the photosynthetic capacity since 2000, when trees were bent as a consequence of the sliding. We found that trees responded to the sliding-induced trauma by adjusting the photosynthetic process and producing compression wood (note that isotopes were analysed only in cores without compression wood; see Methods).

Changes in photosynthetic capacity are not induced solely by geomorphological processes, and the use of at least one control site is mandatory for correctly disentangling the origin of the signals, i.e., climatic vs. geomorphological. In fact, the trees at all sites show higher photosynthetic capacity in years 1987 and 1988, including the control site C, indicating a common response to the same meteorological conditions in the absence geomorphological disturbances. At the control site C, positive correlation between the $\delta^{13}C$ and $\delta^{18}O$ series reflects stable physiological conditions through time, mainly driven by stomatal conductance regulating internal CO_2 concentration and photosynthesis (Cullen et al., 2008). At site C, in the years 1987, 1988 (similarly recorded also at sites A and B), and 1991, high $\delta^{13}C$ and low $\delta^{18}O$ values indicate an acceleration of the photosynthetic capacity due to climatic factors, whereas a deceleration occurs in 2005 and 2006 (Fig. 5B).

Geomorphological processes may alter tree physiology, thus masking the climatic signals in the tree-ring stable isotope series. At site B, the pattern of correlations with climatic variables is often opposite that at the control site C, which is a strong indication of the influence of mass-wasting processes on isotope fractionation. In fact, high temperature and dry air conditions (which are typical of the Mediterranean summer) tend to lower the tree-ring $\delta^{13}C$ at site B, and correspond to periods of decreased photosynthetic capacity at the landslide site. This is very unusual, as a wide range of studies have shown that dry conditions tend to increase $\delta^{13}C$ (e.g., Kress et al., 2010). This decrease in photosynthetic capacity occurs at site B after the onset of the 1993 event and as sudden drops in 2003 and 2011 (see SCOD index changes in Fig. 5B). At control site C, in contrast, the same climatic conditions (dry and hot) tend to increase the $\delta^{13}C$ values as expected in undisturbed sites. This indicates a lower stomatal conductance, but no changes in the photosynthetic capacity are evidenced by the SCOD index (with the exception of the year 2006; Fig. 5B). Site B also shows a markedly different response from the sites A and C with respect to the temperature range variable. Especially during the growing season, an increase in the temperature range tends to result in increased $\delta^{13}C$ values at site B, whereas the opposite occurs at sites A and C. Similarly, precipitation totals only marginally influence the $\delta^{18}O$ at site C, whereas precipitation $\delta^{18}O$ has a more distinct influence. The series for the Porano station was reconstructed based on data from nine stations across the Italian peninsula, but unfortunately the retrieved series were rather short. We found that precipitation $\delta^{18}O$ during the growing season is only linked to tree-ring $\delta^{18}O$ at the control site C. No clear patterns are found at either the landslide site B or at site A, providing another indication of the presence of active geomorphological processes masking the climatic signal.

Considering the importance of the above evidence linking geomorphological processes and tree physiology responses, our approach offers the following advantages in geomorphological applications:

i) it can methodologically support studies aimed at landslide hazard assessment, as the evaluation of the spatial and temporal distribution of past events is often impeded by missing historical records;
ii) it contributes to disentangling the complex relationship between vegetation, climate, and denudation processes.

The studied landscape is highly impacted by interactions between water erosion and landsliding processes, which result in a complex cause-effect relationship (Vergari et al., 2019). This may represent sources of geomorphological hazards, provoking high sediment yields but also disturbance towards vegetation. Castaldi and Chiocchini (2012) studied the effects of reforestation practices on badlands erosion in the area, showing that the remarkable fragmentation, due to the limited presence of suitable areas for tree seedlings, has impeded the formation of continuous forest cover. Tree cover in this landscape plays a crucial role in altering soil properties by enhancing organic matter accumulation and water infiltration to form more stable slope conditions (Vergari et al., 2013a; Bierbaß et al., 2014). However, Vergari et al. (2011) showed that, locally, reforestation has failed to curb slope erosion, as the re-planted trees on the calanchi heads represent an overload that favours landsliding. However, as Gallart et al. (2013) noted, hillslope denudation heavily and permanently impacts tree vegetation, as confirmed by both Bollati et al. (2016) and the results of this study. According to Bollati et al. (2016), the evolution from pure calanchi (type

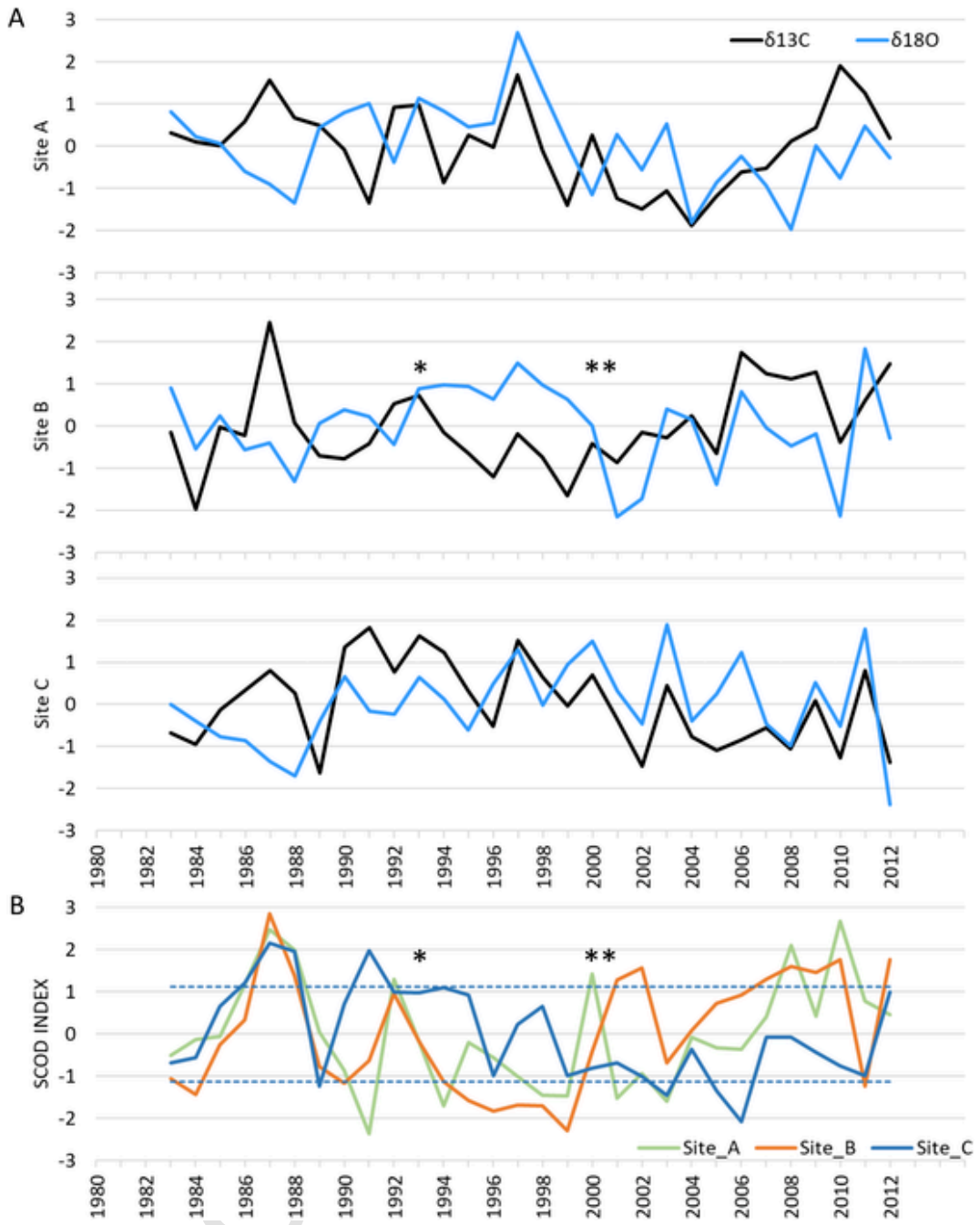

Fig. 5. A) Z-scores of the $\delta^{13}C$ and $\delta^{18}O$ chronologies coupled by sampling site for within-site comparisons. B) SCOD index, which is proportional to the photosynthetic activity calculated at the three sampling sites. Horizontal dashed lines represent $\pm 1\sigma$ of SCOD values at the control site C, over the considered period. The asterisks indicate the events independently identified in Bollati et al. (2016) by means of growth anomalies, compression wood, and root exposure: * indicates the onset of the 1993 event (see Introduction) followed by low photosynthetic rates at site B. ** indicates the onset of the 2000 event followed by a period of higher photosynthetic capacity at site B despite the formation of compression wood.

A) to landslide-affected badlands (type B) was accompanied by an increase in erosion rates. Not only do the physical features of the trees reflect this increase in erosion, but so does the chemical composition of the tree–ring cellulose (namely, the stable isotope content of C and O).

6. Conclusions

To our knowledge, this is the first tree-ring stable isotope analysis in a dendrogeomorphological study. Trees growing on active landslides are directly impacted by the movement of the ground and likely also by changes in soil water content, and adjust their structures and physiology to accommodate the changes. These changes are recorded in their rings and the isotopic signatures of their rings, making it possible to reconstruct geomorphological changes. The use of at least one not-too-distant control site, where same climatic conditions but no geomorphological processes are impacting trees, allows for the reconstruction of the normal physiological conditions and thus, by comparison, for the detection of geomorphological processes at the landslide site. Following a landslide event (in 1993), trees showed an initial period of reduced photosynthetic capacity, followed since 2000 by a period high photosynthetic rates during the intense reaction wood production due to the geomorphological instabilities. In this study, we demonstrate that tree-

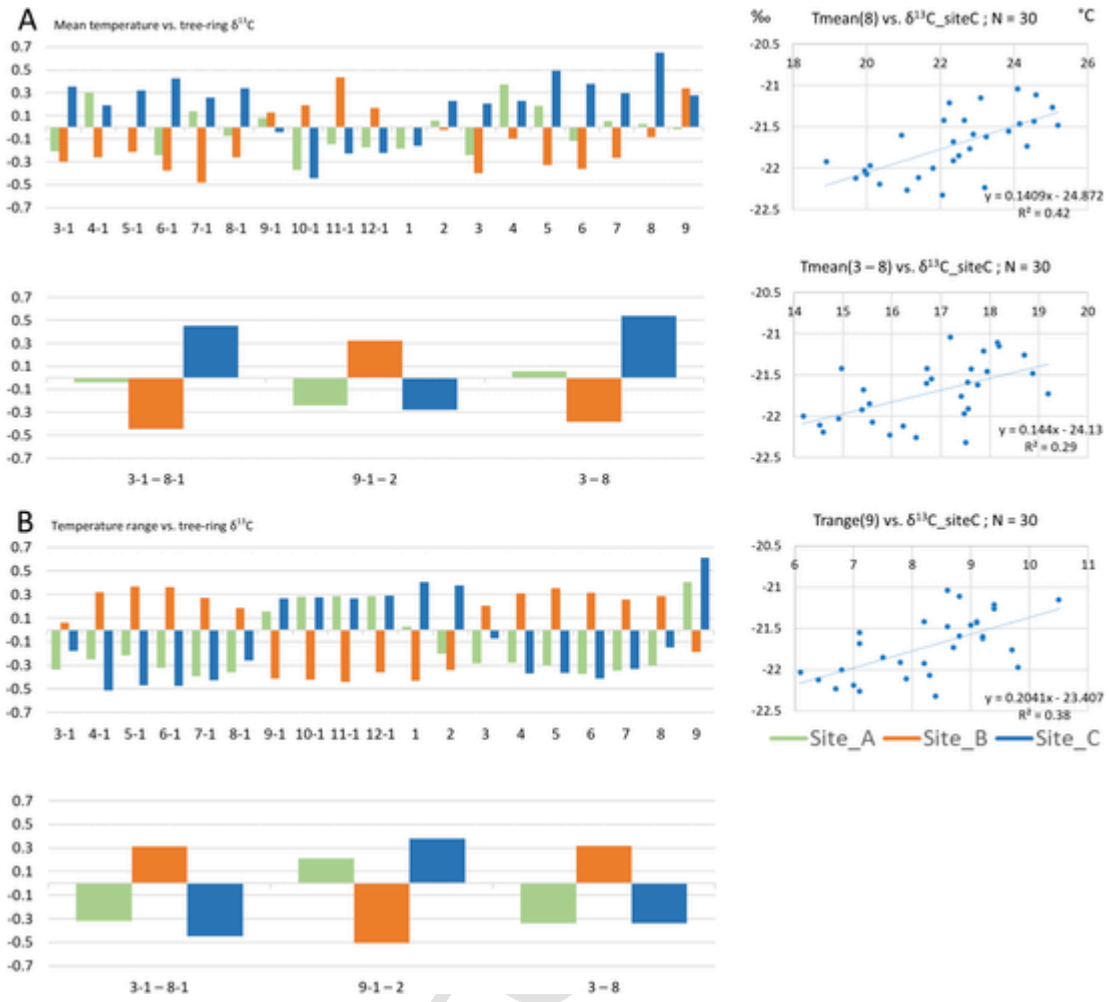

Fig. 6. A) Correlation coefficients calculated between $\delta^{13}C$ chronologies at the tree sampling sites using monthly and seasonal variables of mean temperature over the period 1983–2012 (number months as labels; '−1' indicates a variable in the year prior to growth). Regression plots are shown on the right for monthly or seasonal variables with a correlation coefficient $r > 0.5$ ($p < 0.01$). Regression equations and determination coefficients are also reported. For August (month #8), $r = 0.65$ ($p < 0.001$); for March–August (3–8), $r = 0.54$ ($p < 0.01$). B) Correlation coefficients calculated between $\delta^{13}C$ chronologies vs. monthly and seasonal variables of mean temperature range. For September (9), $r = 0.61$ ($p < 0.001$).

ring stable isotopes can provide valuable information regarding ongoing geomorphological dynamics and can be used as proxy for mass-wasting processes in forested landslides, for tracking ongoing processes on slopes, and for dating landslide events.

Uncited references

Del Prete et al., 1997
Maccherini et al., 2000

CRediT authorship contribution statement

Giovanni Leonelli: Conceptualization, Methodology, Formal analysis, Writing – original draft. **Irene Maria Bollati:** Investigation, Resources, Data curation, Writing – original draft. **Paolo Cherubini:** Investigation, Resources, Writing – review & editing, Supervision. **Matthias Saurer:** Writing – review & editing. **Francesca Vergari:** Investigation, Writing – review & editing. **Maurizio Del Monte:** Supervision, Writing – review & editing. **Manuela Pelfini:** Writing – review & editing, Supervision, Funding acquisition.

Declaration of competing interest

The authors declare the following financial interests/personal relationships which may be considered as potential competing interests: Irene Maria Bollati reports financial support was provided by Government of Italy Ministry of Education University and Research.

Acknowledgments

The Authors acknowledge the anonymous Reviewers who helped us with useful suggestions, Erin Gleeson who revised the English, Dr. E. Menin, Dr. F. Sobacchi, and the students who participated in the sampling and geomorphological surveys in the area and in preparing the samples in the Dendrogeomorphology Laboratory of the Earth Science Department "A. Desio" of the University of Milan. Moreover, the authors thank Dr. E. Valente and Dr. Loic Schneider for assisting with the analyses performed at the WSL laboratories.

Funding

This research was funded by the Ministero Istruzione Università Ricerca (MIUR) Prin 2010–2011 project "Response of morphoclimatic system dynamics to global changes and related geomorphological hazards" (Award Number: 2010AYKTAB_0069). This work has also bene-

Fig. 7. A) Correlation coefficients calculated between $\delta^{18}O$ chronologies at the tree sampling sites using monthly variables of total precipitation over the period 1983–2012. B) Correlation coefficients calculated between $\delta^{18}O$ chronologies vs. monthly and seasonal variables of precipitation $\delta^{18}O$ over the period 1983–2003 (shorter period due to the lack of data in the precipitation series). Regression plots are reported on the right for monthly or seasonal variables showing a correlation coefficient of $r > 0.45$ ($p < 0.05$; at site C) and $r > 0.59$ ($p < 0.01$), respectively. Regression equations and determination coefficients are also reported.

fited from the framework of the COMP-HUB Initiative of the Università di Parma, and from the Università degli Studi di Milano, both funded by the 'Departments of Excellence' program of the Italian Ministry of Education, University and Research (MIUR, 2018–2022).

References

Acocella, V., Rossetti, F., 2002. The role of extensional tectonics at different crustal levels on granite ascent and emplacement: an example from Tuscany (Italy). Tectonophysics 354 (1–2), 71–83. https://doi.org/10.1016/S0040-1951(02)00290-1.

Alestalo, J., 1971. Dendrochronological interpretation of geomorphic processes. Fennia 105, 140.

Alexander, D.E., 1982. Difference between "calanchi" and "biancane" badlands in Italy. In: Bryan, R.B., Yair, A. (Eds.), Badland Geomorphology and Piping. Geobooks, pp. 71–87.

Altieri, S., Mereu, S., Cherubini, P., Castaldi, S., Sirignano, C., Lubritto, C., Battipaglia, G., 2015. Tree-ring carbon and oxygen isotopes indicate different water use strategies in three Mediterranean shrubs at capo caccia (Sardinia, Italy). Trees 29, 1593–1603. https://doi.org/10.1007/s00468-015-1242-z.

Amici, V., Maccherini, S., Santi, E., Torri, D., Vergari, F., Del Monte, M., 2017. Long-term patterns of change in a vanishing cultural landscape: a GIS-based assessment. Ecol. Informatics 37, 38–51. https://doi.org/10.1016/j.ecoinf.2016.11.008.

Arbellay, E., Stoffel, M., Sutherland, E.K., Smith, K.T., Falk, D.A., 2014. Resin duct size and density as ecophysiological traits in fire scars of Pseudotsuga menziesii and Larix occidentalis. Ann. Bot. 114, 973–980. https://doi.org/10.1093/aob/mcu168.

Arosio, T., Ziehmer, M.M., Nicolussi, K., Schlüchter, C., Leuenberger, M., 2020. Alpine holocene tree-ring dataset: age-related trends in the stable isotopes of cellulose show species-specific patterns (preprint). Biogeosciences 17, 4871–4882. https://doi.org/10.5194/bg-17-4871-2020.

Aucelli, P.P., Conforti, M., Della Seta, M., Del Monte, M., Rosskopf, C.M., Vergari, F., D'uva, L., 2016. Multi-temporal digital photogrammetric analysis for quantitative assessment of soil erosion rates in the Landola catchment of the Upper Orcia Valley (Tuscany, Italy). Land Degradation & Development 27 (4), 1075–1092. https://doi.org/10.1002/ldr.2324.

Ballesteros Cánovas, J.A., Bodoque, J.M., Lucía, A., Martín-Duque, J.F., Díez-Herrero, A., Ruiz-Villanueva, V., Rubiales, J.M., Genova, M., 2013. Dendrogeomorphology in badlands: methods, case studies and prospects. Catena 106, 113–122. https://doi.org/10.1016/j.catena.2012.08.009.

Barbehenn, R.V., Constabel, C.P., 2011. Tannins in plant–herbivore interactions. Phytochemistry 72, 1551–1565. https://doi.org/10.1016/j.phytochem.2011.01.040.

Bégin, C., Gingras, M., Savard, M.M., Marion, J., Nicault, A., Bégin, Y., 2015. Assessing tree-ring carbon and oxygen stable isotopes for climate reconstruction in the Canadian northeastern boreal forest. Palaeogeogr. Palaeoclimatol. Palaeoecol. 423, 91–101. https://doi.org/10.1016/j.palaeo.2015.01.021.

Belisario, F., Del Monte, M., Fredi, P., Funiciello, R., Lupia Palmieri, E., Salvini, F., 1999. Azimuthal analysis of stream orientations to define regional tectonic lines. Zeitschrift für Geomorphologie (Suppl.-Bd 118), 41–63.

Beniston, M., 2004. The 2003 heat wave in Europe: A shape of things to come? An analysis based on Swiss climatological data and model simulations. Geophysical Research Letters 31, L02202. https://doi.org/10.1029/2003GL018857.

Bierbaß, P., Wündsch, M., Michalzik, B., 2014. The impact of vegetation on the stability of dispersive material forming biancane badlands in val d'Orcia, Tuscany, Central Italy. Catena 113, 260–266. https://doi.org/10.1016/j.catena.2013.08.003.

Bollati, I., Della Seta, M., Pelfini, M., Del Monte, M., Fredi, P., Palmieri, E.L., 2012. Dendrochronological and geomorphological investigations to assess water erosion and mass wasting processes in the apennines of southern Tuscany (Italy). Catena 90, 1–17. https://doi.org/10.1016/j.catena.2011.11.005.

Bollati, I., Vergari, F., Del Monte, M., Pelfini, M., 2016. Multitemporal dendrogeomorphological analysis of slope instability in upper Orcia Valley (Southern Tuscany, Italy). Geogr. Fis. Din. Quat. 39 (2), 105–120. https://doi.org/10.4461/GFDQ 2016.39.10.

Brandolini, P., Pepe, G., Capolongo, D., Cappadonia, C., Cevasco, A., Conoscenti, C., Marsico, A., Vergari, F., Del Monte, M., 2018. Hillslope degradation in representative italian areas: just soil erosion risk or opportunity for development? Land Degrad. Dev. 29 (9), 3050–3068. https://doi.org/10.1002/ldr.2999.

Buccolini, M., Coco, L., 2013. MSI (morphometric slope index) for analyzing activation and evolution of calanchi in Italy. Geomorphology 191, 142–149. https://doi.org/10.1016/j.geomorph.2013.02.025.

Carmignani, L., Decandia, F.A., Fantozzi, P.L., Lazzarotto, A., Liotta, D., Meccheri, M., 1994. Tertiary extensional tectonics in Tuscany (Northern apennines, Italy). Tectonophysics 238, 295–315. https://doi.org/10.1016/0040-1951(94)90061-2.

Castaldi, F., Chiocchini, U., 2012. Effects of land use changes on badland erosion in clayey drainage basins, radicofani, Central Italy. Geomorphology 169–170, 98–108. https://doi.org/10.1016/j.geomorph.2012.04.016.

Chiarucci, A., De Dominicis, V., Ristori, J., Calzolari, C., 1995. Biancana badland vegetation in relation to morphology and soil in Orcia ValleyCentral Italy. Phytocoenologia 25 (1), 69–87. https://doi.org/10.1127/phyto/25/1995/69.

Ciccacci, S., Del Monte, M., Marini, R., 2003. Erosion and recent morphological change in a sample area of the Orcia River Upper Basin (Southern Tuscany). Geogr. Fis. Din. Quat. 26, 97–109.

Ciccacci, S., Galiano, M., Roma, M.A., Salvatore, M.C., 2008. Morphological analysis and erosion rate evaluation in badlands of radicofani area (Southern Tuscany—Italy). Catena 74, 87–97. https://doi.org/10.1016/j.catena.2008.03.012.

Clarke, M.L., Rendell, H.M., 2006. Process–form relationships in southern italian

badlands: erosion rates and implications for landform evolution. Earth Surf. Process. Landf. 31, 15–29. https://doi.org/10.1002/esp.1226.
Cullen, L.E., Adams, M.A., Anderson, M.J., Grierson, P.F., 2008. Analyses of δ13C and δ18O in tree rings of Callitris columellaris provide evidence of a change in stomatal control of photosynthesis in response to regional changes in climate. Tree Physiol. 28, 1525–1533. https://doi.org/10.1093/treephys/28.10.1525.
De Micco, V., Saurer, M., Aronne, G., Tognetti, R., Cherubini, P., 2007. Variations of wood anatomy and δ13C within tree rings of coastal Pinus pinaster showing intra-annual density fluctuations. IAWA J. 28 (1), 61–74.
De Micco, V., Campelo, F., De Luis, M., Bräuning, A., Grabner, M., Battipaglia, G., Cherubini, P., 2016. Intra-annual density fluctuations in tree rings: how, when, where, and why? IAWA J. 37 (2), 232–259.
Del Monte, M., Vergari, F., Brandolini, P., Capolongo, D., Cevasco, A., Ciccacci, S., Conoscenti, C., Fredi, P., Melelli, L., Rotigliano, E., Zucca, F., 2015. Multi-method evaluation of denudation rates in small Mediterranean catchments. In: Lollino, G., Manconi, A., Clague, J., Shan, W., Chiarle, M. (Eds.), Engineering Geology for Society and Territory Volume 1 Climate Change and Engineering Geology. Springer, pp. 563–567.
Del Prete, M., Bentivenga, M., Amato, M., Basso, F., Tacconi, P., 1997. Badland erosion processes and their interactions with vegetation: a case study from pisticci, Basilicata, southern Italy. Geogr. Fis. Din. Quat. 20, 147–155.
Della Seta, M., Del Monte, M., Fredi, P., Palmieri, E.L., 2009. Space–time variability of denudation rates at the catchment and hillslope scales on the tyrrhenian side of Central Italy. Geomorphology 107, 161–177. https://doi.org/10.1016/j.geomorph.2008.12.004.
Di Matteo, G., De Angelis, P., Brugnoli, E., Cherubini, P., Scarascia Mugnozzza, G., 2010. Tree-ring Δ13C reveals the impact of past forest management on water-use efficiency in a Mediterranean oak coppice in Tuscany (Italy). Ann. For. Sci. 67 (5), 510. https://doi.org/10.1051/forest/2010012.
Farquhar, G.D., Ehleringer, J.R., Kubick, K.T., 1989. Carbon isotope discrimination and photosynthesis. Annu. Rev. Plant Physiol. Plant Mol. Biol. 40, 503–537.
Gallart, F., Solé, A., Puigdefábregas, J., Lázaro, R., 2002. Badland systems in the Mediterranean. In: Bull, L.J., Kirkby, M.J. (Eds.), Dryland Rivers: Hydrology and Geomorphology of Semi-arid Channels. John Wiley & Sons, pp. 299–326.
Gallart, F., Marignani, M., Pérez-Gallego, N., Santi, E., Maccherini, S., 2013. Thirty years of studies on badlands, from physical to vegetational approaches. A succinct review. Catena 106, 4–11. https://doi.org/10.1016/j.catena.2012.02.008.
Herms, D.A., Mattson, W.J., 1992. The dilemma of plants: to grow or defend. The Quarterly Review Of Biology 67, 283–35.
Hogg, E.H., Hart, M., Lieffers, V.J., 2002. White tree rings formed in trembling aspen saplings following experimental defoliation. Can. J. For. Res. 32, 1929–1934. https://doi.org/10.1139/x02-114.
IAEA/WMO, 2021. Global Network of Isotopes in Precipitation. The GNIP Database Accessible at. http://www.iaea.org/water.
Klesse, S., Weigt, R., Treydte, K., Saurer, M., Schmid, L., Siegwolf, R.T.W., Frank, D.C., 2018. Oxygen isotopes in tree rings are less sensitive to changes in tree size and relative canopy position than carbon isotopes. Plant Cell Environ. 41, 2899–2914. https://doi.org/10.1111/pce.13424.
Kress, A., Saurer, M., Siegwolf, R.T.W., Frank, D.C., Esper, J., Bugmann, H., 2010. A 350 year drought reconstruction from alpine tree ring stable isotopes. Glob. Biogeochem. Cycles 24 (2), GB2011. https://doi.org/10.1029/2009GB003613.
Leonelli, G., Battipaglia, G., Siegwolf, R.T.W., Saurer, M., Morra di Cella, U., Cherubini, P., Pelfini, M., 2012. Climatic isotope signals in tree rings masked by air pollution: a case study conducted along the Mont Blanc tunnel access road (Western Alps, Italy). Atmos. Environ. 61, 169–179. https://doi.org/10.1016/j.atmosenv.2012.07.023.
Liotta, D., 1996. Analisi del settore centromeridionale del bacino pliocenico di radicofani (Toscana meridionale). Boll. Soc. Paleontol. Ital. 115, 115–143.
Loader, N.J., Robertson, I., Barker, A.C., Switsur, V.R., Waterhouse, J.S., 1997. An improved technique for the batch processing of small whole wood samples to alpha-cellulose. Chem. Geol. 136, 313–317. https://doi.org/10.1016/S0009-2541(96)00133-7.
Longinelli, A., Anglesio, E., Flora, C., Iacumin, P., Selmo, E., 2006. Isotopic composition of precipitation in northern Italy: reverse effect of anomalous climatic events. J. Hydrol. 329, 471–476. https://doi.org/10.1016/j.jhydrol.2006.03.002.
Maccherini, S., Chiarucci, A., De Dominicis, V., 2000. Structure and species diversity of Bromus erectus grasslands of biancana badlands. Belg. J. Bot. 133, 3–14. https://doi.org/10.2307/20794459.
McCarroll, D., Loader, N.J., 2004. Stable isotopes in tree rings. Quat. Sci. Rev. 23, 771–801. https://doi.org/10.1016/j.quascirev.2003.06.017.
Moretti, S., Rodolfi, G., 2000. A typical "calanchi" landscape on the eastern apennine margin (Atri, Central Italy): geomorphological features and evolution. Catena 40, 217–228. https://doi.org/10.1016/S0341-8162(99)00086-7.
Nadal-Romero, E., Rodríguez-Caballero, E., Chamizo, S., Juez, C., Cantón, Y., García-Ruiz, J.M., 2021. Mediterranean badlands: their driving processes and climate change futures. Earth Surf. Process. Landf. 1–15. https://doi.org/10.1002/esp.5088.
Nagavciuc, V., Ionita, M., Perşoiu, A., Popa, I., Loader, N.J., McCarroll, D., 2019. Stable oxygen isotopes in romanian oak tree rings record summer droughts and associated large-scale circulation patterns over Europe. Clim. Dyn. 52, 6557–6568. https://doi.org/10.1007/s00382-018-4530-7.
Neugirg, F., Stark, M., Kaiser, A., Vlacilova, M., Della Seta, M., Vergari, F., Schmidtb, J., Bechta, M., Haas, F., 2016. Erosion processes in calanchi in the upper Orcia Valley, southern Tuscany, Italy based on multitemporal high-resolution terrestrial LiDAR and UAV surveys. Geomorphology 269, 8–22. https://doi.org/10.1016/j.geomorph.2016.06.027.
Payomrat, P., Liu, Y., Pumijumnong, N., Li, Q., Song, H., 2018. Tree-ring stable carbon isotope-based June–September maximum temperature reconstruction since AD 1788, north-West Thailand. Tellus B Chem. Phys. Meteorol. 70, 1–13. https://doi.org/10.1080/16000889.2018.1443655.
Roden, J., Siegwolf, R.T.W., 2012. Is the dual-isotope conceptual model fully operational? Tree Physiol. 32, 1179–1182. https://doi.org/10.1093/treephys/tps099.
Saurer, M., Borella, S., Leuenberger, M., 1997. δ18O of tree rings of beech (Fagus sylvatica) as a record of δ18O of the growing season precipitation. Tellus B Chem. Phys. Meteorol. 49, 80–92. https://doi.org/10.3402/tellusb.v49i1.15952.
Saurer, M., Cherubini, P., Siegwolf, R.T.W., 2000. Oxygen isotopes in tree rings of Abies alba: the climatic significance of interdecadal variations. J. Geophys. Resour. 105 (D10), 12461–12470. https://doi.org/10.1029/2000JD900160.
Saurer, M., Kirdyanov, A.V., Prokushkin, A.P., Rinne, K.T., Siegwolf, R.T.W., 2016. The impact of an inverse climate–isotope relationship in soil water on the oxygen-isotope composition of Larix gmelinii in Siberia. New Phytol. 209, 955–964. https://doi.org/10.1111/nph.13759.
Savard, M.M., 2010. Tree-ring stable isotopes and historical perspectives on pollution –an overview. Environ. Pollut. 158, 2007–2013. https://doi.org/10.1016/j.envpol.2009.11.031.
Savard, M.M., Daux, V., 2020. An overview on isotopic divergences – causes for instability of tree-ring isotopes and climate correlations. Clim. Past 16, 1223–1243. https://doi.org/10.5194/cp-16-1223-2020.
Savard, M.M., Bégin, C., Marion, J., 2020. Response strategies of boreal spruce trees to anthropogenic changes in air quality and rising pCO2. Environ. Pollut. 114209. https://doi.org/10.1016/j.envpol.2020.114209.
Scheidegger, K.Y., Saurer, M., Bahn, M., Siegwolf, R.T.W., 2000. Linking stable oxygen and carbon isotopes with stomatal conductance and photosynthetic capacity: a conceptual model. Oecologia 125, 350–357. https://doi.org/10.1007/s004420000466.
Schweingruber, F.H., 1996. In: dendroecology. Paul Haupt AG Bern (Ed.), Tree rings and environment. p. 609 pp.
Sensuła, B.M., 2015. Spatial and short-temporal variability of δ13c and δ15n and water-use efficiency in pine needles of the three forests along the most industrialized part of Poland. Water Air Soil Pollut. 226, 362. https://doi.org/10.1007/s11270-015-2623-z.
Shigo, A.L., 1984. Compartmentalization: a conceptual framework for understanding how trees grow and defend themselves. Annu. Rev. Phytopathol. 22, 189–214.
Smith, K.T., 2015. Compartmentalization, resource allocation, and wood quality. Curr. For. Rep. 1, 8–15. https://doi.org/10.1007/s40725-014-0002-4.
Stoffel, M., Corona, C., 2014. Dendroecological dating of geomorphic disturbance in trees. Tree Ring Res. 70 (1), 3–20. https://doi.org/10.3959/1536-1098-70.1.3.
Sutton, A., Tardif, J., 2005. Distribution and anatomical characteristics of white rings in Populus tremuloides. IAWA J. 26 (2), 221–238.
Thornes, J.B., 1985. The ecology of erosion. Geography 70, 222–235. https://doi.org/10.1177/0309133310367548.
Tognetti, R., Lombardi, F., Lasserre, B., Cherubini, P., Marchetti, M., 2014. Tree-ring stable isotopes reveal twentieth-century increases in water-use efficiency of Fagus sylvatica and Nothofagus spp. in Italian and Chilean mountains. PLoS One 9 (11), e113136. https://doi.org/10.1371/journal.pone.0113136.
Torri, D., Regüés, D., Pellegrini, S., Bazzoffi, P., 1999. Within-storm soil surface dynamics and erosive effects of rainstorms. Catena 38, 131–150.
Torri, D., Santi, E., Marignani, M., Rossi, M., Borselli, L., Maccherini, S., 2013. The recurring cycles of biancana badlands: erosion, vegetation and human impact. Catena 106, 22–30. https://doi.org/10.1016/j.catena.2012.07.001.
Treydte, K., Schleser, G.H., Schweingruber, F.H., Winiger, M., 2001. The climatic significance of δ13C in subalpine spruces (Lötschental, swiss Alps). Chem. Phys. Meteorol. 53, 593–611. https://doi.org/10.3402/tellusb.v53i5.16639.
Treydte, K.S., Schleser, G.H., Helle, G., Frank, D.C., Winiger, M., Haug, G.H., Esper, J., 2006. The twentieth century was the wettest period in northern Pakistan over the past millennium. Nature 440, 1179–1182. https://doi.org/10.1038/nature04743.
Treydte, K., Boda, S., Graf Pannatier, E., Fonti, P., Frank, D., Ullrich, B., Saurer, M., Siegwolf, R.T.W., Battipaglia, G., Werner, W., Gessler, A., 2014. Seasonal transfer of oxygen isotopes from precipitation and soil to the tree ring: source water versus needle water enrichment. New Phytology 202, 772–783. https://doi.org/10.1111/nph.12741.
Vergari, F., Della Seta, M., Del Monte, M., Fredi, P., Palmieri, E.L., 2011. Landslide susceptibility assessment in the upper Orcia Valley (Southern Tuscany, Italy) through conditional analysis: a contribution to the unbiased selection of causal factors. Nat. Hazards Earth Syst. Sci. 11, 1475–1497. https://doi.org/10.5194/nhess-11-1475-2011.
Vergari, F., Della Seta, M., Del Monte, M., Barbieri, M., 2013a. Badlands denudation "hot spots": the role of parent material properties on geomorphic processes in 20-years monitored sites of southern Tuscany (Italy). Catena 106, 31–41. https://doi.org/10.1016/j.catena.2012.02.007.
Vergari, F., Della Seta, M., Del Monte, M., Fredi, P., Palmieri, E.L., 2013b. Long-and short-term evolution of several Mediterranean denudation hot spots: the role of rainfall variations and human impact. Geomorphology 183, 14–27. https://doi.org/10.1016/j.geomorph.2012.08.002.
Vergari, F., Troiani, F., Faulkner, H., Del Monte, M., Della Seta, M., Ciccacci, S., Fredi, P., 2019. The use of the slope–area function to analyse process domains in complex badland landscapes. Earth Surf. Process. Landf. 44, 273–286. https://doi.org/10.1002/esp.4496.
Weigt, R.M., Bräunlich, S., Zimmermann, L., Saurer, M., Grams, T.E.E., Dietrich, H.P., Siegwolf, R.T.W., Nikolova, P.S., 2015. Comparison of δ18O and δ13C values between tree-ring whole wood and cellulose in five species growing under two different site conditions. Rapid Commun. Mass Spectrom. 29, 2233–2244. https://doi.org/10.1002/rcm.7388.